

Influence of Conformation and Intramolecular Hydrogen Bonding on the Acyl Glucuronidation and Biliary Excretion of Acetylenic Bis-Dipyrrinones Related to Bilirubin

Antony F. McDonagh^{*,†} and David A. Lightner[‡]

Division of Gastroenterology, University of California, San Francisco, California 94143-0538, and Department of Chemistry, University of Nevada, Reno, Nevada 89557-0020

Received August 5, 2006

Glucuronidation and transporter-mediated efflux into bile are important in the elimination of xeno- and endobiotics, including the natural biladienone pigment bilirubin. The mechanisms of these processes and the structural factors that dictate whether cholephilic compounds are excreted directly in bile or require prior glucuronidation are poorly understood. To investigate effects of molecular shape and intramolecular hydrogen bonding on the interplay between direct excretion and glucuronidation in the liver, we studied a series of novel synthetic exploded and homologated bilirubin analogues. These include dicarboxylic mono- and diacetylenic tetrapyrroles with linear shapes that are unable to adopt the folded ridge–tile conformations that are crucially important in bilirubin metabolism. Intramolecular hydrogen bonding was varied by adjusting the alkyl chain lengths of the pendent carboxyl groups, and preferred conformations were predicted by molecular dynamics calculations. Metabolism studies were done in rats, including Gunn rats, congenitally deficient in UGT1 glucuronosyl transferases, and TR⁻ rats, deficient in the canalicular transporter Mrp2 (Abcc2). The results show strikingly that minor, seemingly inconsequential, changes in constitution, amplified by their influence on hydrogen bonding and molecular conformation, can profoundly influence competing clearance pathways in the liver, an effect that is unlikely to be restricted to bis-dipyrrinone carboxylic acids. Exposed carboxyl groups seem to favor the direct route of elimination, whereas the potential for carboxyl infolding by hydrogen bonding seems to favor glucuronidation. The results also show that molecular shape is less important in the hepatic glucuronidation and biliary excretion of bilirubin and of this series of acids than the capacity for intramolecular hydrogen bonding.

Introduction

The fundamental importance of inter- and intramolecular hydrogen bonding in molecular biology and supramolecular chemistry is well-known, as is the potential influence of intramolecular hydrogen bonding on the physicochemical properties of molecules. However, the influence of intramolecular hydrogen bonding on the hepatic uptake, metabolism, and biliary excretion of medium molecular weight xenobiotics has been less well studied, though it is thought to be particularly important in the biochemistry of cyclosporin¹ and of the naturally occurring pigment bilirubin.² Bilirubin (**1**, Figure 1) is a neurotoxic antioxidant produced in mammals and some nonmammalian vertebrates by reduction of biliverdin (**2**) generated during normal red cell and heme catabolism. It is a prototypical substrate for the phase 2 glucuronosyl transferase enzyme UGT1A1,^{a,3} and its three acylglucuronide conjugates, which are its principal metabolites in mammals, are prototypical allocrites⁴ for the canalicular ATP-binding cassette protein MRP2 (multidrug-resistance-associated protein 2, ABCC2).^{5–7} When hepatic excretion of bilirubin is impaired, jaundice and brain damage may result, particularly in newborn babies.²

Conjugation is essential for efficient biliary elimination of bilirubin. Unconjugated bilirubin is not excreted significantly in bile or urine and does not seem to be transported by organic

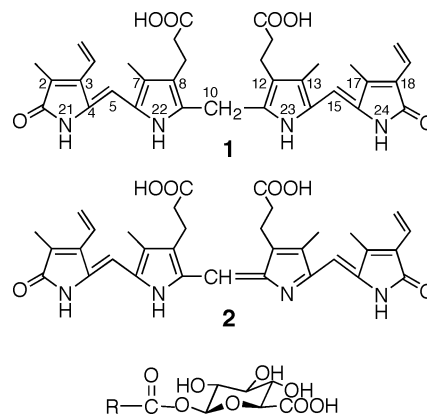


Figure 1. Constitutional structures of bilirubin (**1**) and biliverdin (**2**) and generic structure of an acylglucuronide of a carboxylic acid, RCOOH.

anion transporters present in the biliary canalicular membrane of hepatocytes. Since bilirubin is an aliphatic dicarboxylic acid, this is surprising, particularly when comparison is made to biliverdin (**2**). Biliverdin (didehydrobilirubin) has a similar constitution and acidity to bilirubin,¹² yet is excreted readily in bile in unconjugated form and has not been observed to form glucuronide conjugates *in vivo*.¹³ The apparently anomalous behavior of bilirubin is thought to be rooted in its ability to adopt conformations that favor intramolecular hydrogen bonding involving the carboxyl (carboxylate) groups and enhance its lipophilicity relative to biliverdin. Whereas biliverdin is forced to adopt a helical (lock washer) conformation because of the trigonal –CH– group at C10, the tetrahedral –CH₂– group at C10 in bilirubin allows the linked planar dipyrrinone chromophores to rotate independently into conformations in which

* To whom correspondence should be addressed. Phone: 415-476-6425. Fax: 415-476-0659. E-mail: tony.mcdonagh@ucsf.edu.

[†] University of California.

[‡] University of Nevada.

^a Abbreviations: ABC (Abc, rodent), ATP-binding cassette; MRP2 (Mrp2, rodent), multidrug resistance associated protein 2; UGT, uridine diphosphoglucuronosyl transferase; UGT1A1, uridine diphosphoglucuronosyl transferase 1 family, polypeptide A1.

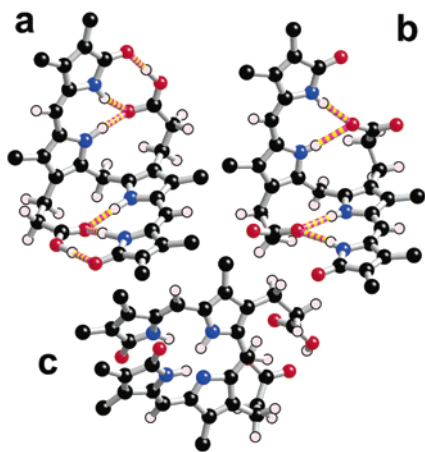


Figure 2. Preferred conformations of (a) bilirubin (**1**), (b) its dianion, and (c) biliverdin (**2**). Some hydrogen atoms and side chain carbons have been omitted for clarity. Striped bonds represent hydrogen bonds. The drawings of bilirubin free acid and its dianion are based on the crystal structure coordinates;^{8,9} for the dianion, two diisopropylammonium counter ions that engage in hydrogen bonding to the carboxylate and lactam oxygens of each dipyrinone are not shown. The structure of biliverdin is based on Sybyl calculations and is similar to that seen in biliprotein crystals.^{10,11}

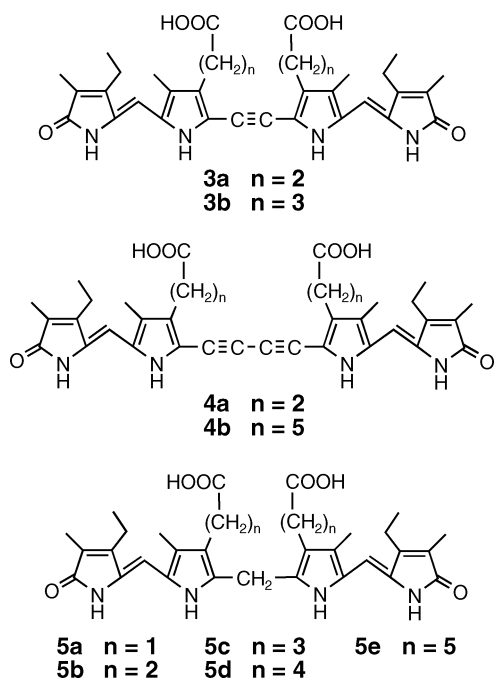


Figure 3. Constitutional structures of compounds used in this study.

they are hydrogen-bonded to carboxyl groups and less exposed to solvent than those in biliverdin (Figure 2). These conformers, often referred to as ridge–tile conformers,⁸ are thought to be of overriding importance in bilirubin metabolism and toxicity. Consistent with this view, several isomers and analogues of bilirubin in which the carboxyl groups are sterically unable to participate in intramolecular hydrogen bonding have been shown to be excreted efficiently in bile in rats without the need for glucuronidation when administered intravenously.^{14,15}

To investigate the inter-related roles of hydrogen bonding and conformation on hepatic metabolism more systematically, we have studied two novel groups of molecular probes containing two dipyrinones and two carboxyl side chains. These include the four homologous “exploded”¹⁶ bilirubin analogues (**3a,b** and **4a,b** in Figure 3), in which the chromophores are separated by linear monoacetylenic and diacetylenic links in

place of the normal $-\text{CH}_2-$ linkage,^{17,18} and a second group, based on bilirubin, containing homologated carboxyl side chains (**5a–e**, Figure 3). The acetylenic compounds are deeply colored, fluorescent, and solvatochromic. Unable to form the folded conformations that are characteristic of natural bilirubin, they are flatter and longer because of the linear hybridization of their $-\text{C}\equiv\text{C}-$ linkages. Nonetheless, their carboxyl side chains can still participate to different degrees in intramolecular hydrogen bonding. Formally, all of the model compounds studied are related to the synthetic pigment mesobilirubin XIII α (**5b**, Figure 3), which has a constitutional and three-dimensional structure similar to bilirubin and undergoes similar metabolism.¹⁹ On the basis of the usual two-dimensional representations shown in Figure 3, little difference in metabolism between **3a** and **3b** and between **4a** and **4b** would be expected. Herein, we compare their hepatobiliary metabolism and biliary excretion in the rat with that of mesobilirubin XIII α and homologues of mesobilirubin XIII α bearing carboxyl side chains of different lengths (**5a,c–e**),²⁰ using Gunn rats, which are congenitally deficient in UGT1A isozymes and are unable to glucuronidate bilirubin;^{21,22} normal wild-type (Sprague-Dawley) rats; and TR⁻ rats, which lack Mrp2 and show impaired biliary excretion of bilirubin glucuronides.^{23,24} The studies reveal striking differences in the hepatic disposition of the four acetylenic bilirubins (**3a,b** and **4a,b**), which are paralleled by marked differences in the metabolism of mesobilirubins **5a–e**. The differences correlate well with the most stable conformations predicted by molecular dynamics calculations and the ability of their pendent carboxyl (carboxylate) groups to engage in intramolecular hydrogen bonding. The results show how seemingly minor changes in constitution can have major effects on metabolism and efflux processes, which might not be apparent from studies *in vitro* using recombinant enzymes or microsomes, and demonstrate the important role that conformation and hydrogen bonding can play in hepatobiliary drug clearance.

Results

Monoacetylenic Bilirubins 3a and 3b.¹⁷ Compounds **3a** and **3b** are homologues of bilirubin (**1**) and mesobilirubin XIII α (**5b**). Their central alkyne linkage prevents them from adopting the characteristic ridge–tile shape that is characteristic of bilirubin and mesobilirubin XIII α (Figure 4, top). Nevertheless, rotation about the alkyne single bonds is possible permitting the two attached, almost planar, dipyrinone chromophores to rotate with respect to each other and generate an infinite number of possible conformations. In some of these, the side chain COOH of one chromophore and the O and NH groups of the other chromophore are juxtaposed. The preferred conformations of bilirubin and mesobilirubin XIII α determined by molecular mechanics force field calculations have been shown to be similar to those of the pigments in the crystalline state (determined by X-ray diffraction), in organic solvents (determined by NMR spectroscopy), and computed by molecular orbital calculations.²⁵ Calculations on **3a** indicate that its global minimum energy conformation is a flat structure (Figure 4, center) in which just one of the two COOH groups is engaged in tight intramolecular hydrogen bonding. Hydrogen bonding of this propionyl COOH exerts enough torque on its attached dipyrinone chromophore to preclude similar hydrogen bonding of the other propionyl COOH.¹⁷ Thus, although **3a** has two propanoic acid side chains as in bilirubin and mesobilirubin XIII α , it differs from these two pigments in that both of its carboxyl groups are unlikely to be strongly hydrogen-bonded simultaneously.

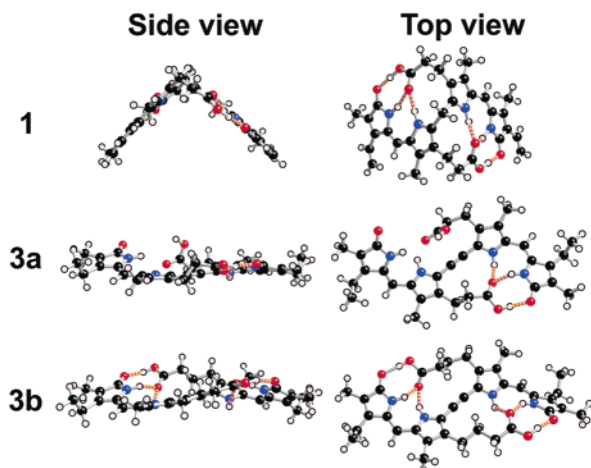


Figure 4. Ball-and-stick representations of global minimum energy conformations of bilirubin (**1**) and monoacetylene mesobilirubins **3a** (propanoic acid side chains) and **3b** (butanoic acid side chains). For convenience, structures of the free acids are shown and discussed, even though these compounds are likely to be ionized in vivo. However, crystallography of bilirubin and its diisopropylammonium salt has shown that the two have similar conformations (Figure 2) with the carboxylate groups in the latter hydrogen-bonded to dipyrinone NH groups.^{8,9} Striped bonds represent hydrogen bonds.

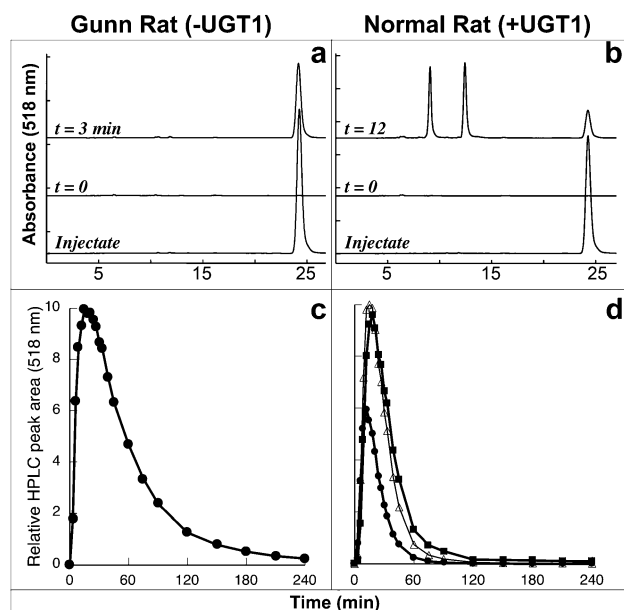


Figure 5. Hepatic metabolism and biliary excretion of **3a** in Gunn and normal rats: (a) HPLC of bile collected just before ($t = 0$) and 3 min after intravenous injection of **3a** (~ 0.25 mg) in a Gunn rat; (b) chromatograms of bile collected before and 12 min after similar injection in a Sprague-Dawley rat; (c) concentration/time excretion curve for **3a** in bile in the Gunn rat (mean of two experiments); (d) similar curves for the excretion of **3a** and its mono- and diglucuronide in Sprague-Dawley rats (mean of three experiments); (●) unchanged **3a**; (Δ) **3a** monoglucuronide; (■) **3a** diglucuronide. Each set of biliary excretion curves is normalized ($\times 10$) to the peak area of the largest HPLC peak.

Injected into UGT1A1-deficient Gunn rats, **3a** was eliminated rapidly in bile unchanged (Figure 5a,c), quite unlike bilirubin and mesobilirubin XIII α , which are not excreted significantly under similar conditions. Intact **3a** was detectable in bile < 3 min after injection, and in duplicate experiments $\sim 93\%$ and 73% of the injected dose was excreted in bile within 240 min. Thus, **3a**, in contrast to bilirubin and mesobilirubin XIII α with similar propanoic acid side chains, is highly cholephilic and

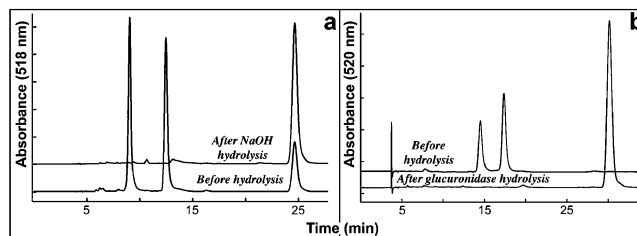


Figure 6. Hydrolysis of metabolites of **3a** and **3b**: (a) HPLC of bile from a Sprague-Dawley rat injected with **3a** before and after hydrolysis with NaOH (similar results obtained with β -glucuronidase); (b) HPLC of bile from a Sprague-Dawley rat injected with **3b** before and after hydrolysis with β -glucuronidase (similar results obtained with NaOH). Chromatograms in panels a and b were run using the same solvent, flow rate, and type of column but on different instruments with different columns.

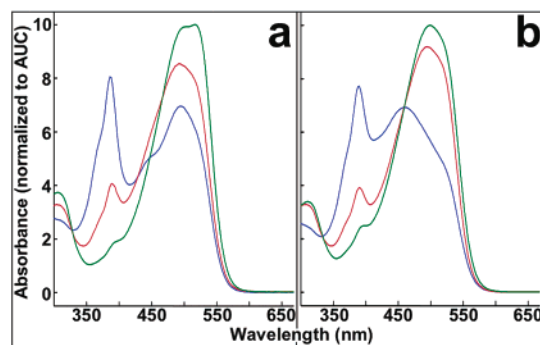
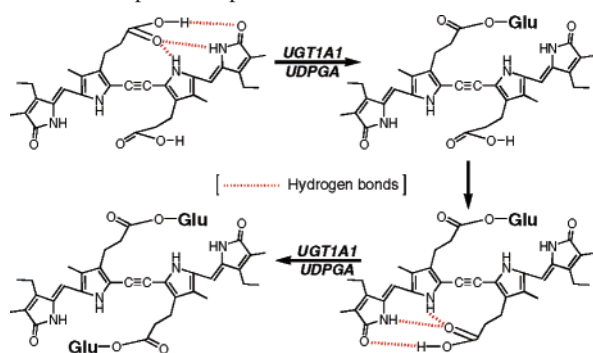


Figure 7. Absorbance spectra of (a) **3a** (green), **3a**-mono-glucuronide (red), and **3a**-di-glucuronide (blue); (b) **3b** (green), **3b**-mono-glucuronide (red), and **3b**-di-glucuronide (blue). Spectra were captured during HPLC of bile samples and normalized to the area under each curve between 350 and 600 nm (solvent, 0.1 M methanolic di-*n*-octylamine acetate containing 5% H₂O). The HPLC peak for **3b**-di-glucuronide overlapped one of the endogenous bilirubin mono-glucuronide peaks. The diglucuronide spectrum depicted in panel b (blue) is therefore distorted by a contribution from bilirubin mono-glucuronide, accounting for some enhanced absorbance at ~ 450 nm.

does not require phase 2 metabolism (glucuronidation) for efficient excretion in bile.

However, when **3a** was injected into normal rats, only part of the injected dose was excreted unchanged in bile, the remainder being converted into two faster-eluting metabolites (Figure 5b,d). On treatment of bile samples with NaOH (Figure 6a) or with β -glucuronidase (not shown), the metabolite peaks disappeared with a concomitant increase in the peak area of unchanged **3a**, confirming the identity of the metabolites as acylglucuronides formed by UGT1 (presumably UGT1A1) catalysis. In view of the order of elution of bilirubin glucuronides (diglucuronide more polar than the monoglucuronides), the faster eluting metabolite is most likely **3a**-diglucuronide and the slower eluting metabolite is **3a**-mono-glucuronide. Glucuronidation caused marked changes in pigment absorbance (Figure 7a), which were consistent with the peak assignments. There was a progressive decline in the absorbance of the main broad band at ~ 480 – 530 nm along with a pronounced increase in absorbance at ~ 390 nm with glucuronidation, suggestive of a major change in the conformational composition of the chromophore. Our data do not distinguish which of the two propanoic acid groups in the preferred conformation of **3a** is first glucuronidated, but we suppose that it is the hydrogen-bonded one. Glucuronidation would be expected to disrupt the erstwhile internal hydrogen bonding present in that half of the molecule and allow the formerly exposed carboxyl group to adopt a potentially hydrogen-bonded conformation (as shown by Dreiding molecular models),

Scheme 1. Proposed Steps in Glucuronidation of **3a**

making it a better substrate for UGT1A1 and facilitating further glucuronidation to give the diglucuronide (Scheme 1).

If this rationalization is correct, lengthening the carboxyl chains of **3a**, as in **3b**, should generate an analogue in which both carboxyl groups can be hydrogen-bonded simultaneously. The molecule would then be expected to mimic bilirubin and mesobilirubin XIII α in its metabolism, despite the longer carboxyl side chains. Consistent with this, molecular dynamics calculations on **3b**, in which each of the propanoic acid side chains of **3a** has been lengthened by just one $-\text{CH}_2-$ group, reveal, as the global energy minimum, a flattish structure in which both carboxyl groups are tightly hydrogen-bonded (Figure 4, bottom).¹⁷ When **3b** was injected into Gunn rats, no significant excretion into bile was observed within 2 h (Figure 8a). But when injected into normal rats, two metabolites (and no parent compound) were excreted rapidly in bile (Figure 8b,c). These metabolites were confirmed to be acylglucuronides, presumably the mono- and diglucuronide, by β -glucuronidase (Figure 6b) and NaOH hydrolysis (not shown). Thus, in contrast to **3a**, the homologue **3b** is metabolized exactly like bilirubin and mesobilirubin XIII α in the rat. Glucuronidation of **3b** induces marked changes in absorbance (Figure 7b) that resemble those seen with **3a** (Figure 7a).

The ABC transporter Mrp2 (Abcc2) is required for efflux of the glucuronides of bilirubin⁶ and mesobilirubin XIII α in bile. This also appears to be true for the glucuronides of **3a** and **3b**. When **3a** was administered to adult male TR⁻ rats (which lack Mrp2), only trace amounts of its glucuronides and unchanged **3a** appeared in bile. When **3b** was similarly administered, its monoglucuronide and diglucuronide were detectable in bile but at a much lower concentration than similar treatment of normal wild-type rats (data not shown). Clearly, **3a** and the glucuronides of **3a** and **3b**, like those of bilirubin and mesobilirubin XIII α , require Mrp2 for efficient hepatic excretion into bile.

Mesobilirubin XIII α Homologues. Our findings on the monoacetylene bilirubins **3a** and **3b** showed that shortening the butanoic acid side chain of **3b** to give **3a** converts the compound from one for which glucuronidation is obligatory for excretion in bile to one that is excretable without glucuronidation. To determine whether the same effect occurs with classical bilirubin structures containing a central $-\text{CH}_2-$ bridge, we studied the biliary excretion of a series of mesobilirubin XIII α homologues (Figure 3) in which each of the normal propanoic acid side chains has been shortened by one carbon unit (**5a**) or lengthened by up to three carbon units (**5c–e**).

Molecular dynamics force field calculations on **5a** (Figure 3), in which the carboxyl side chains are each one methylene unit shorter than in mesobilirubin XIII α , show the lowest energy conformation to be a ridge-tile structure similar to that of bilirubin but with a slightly wider pitch and with both carboxyls

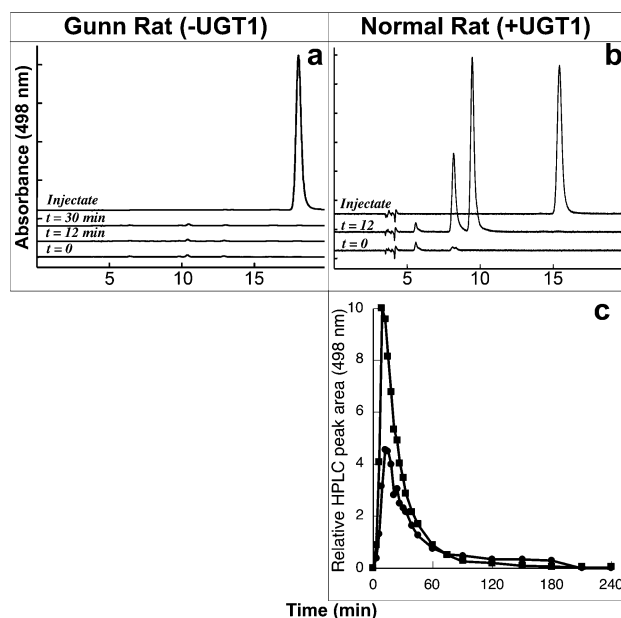


Figure 8. Hepatic metabolism and biliary excretion of **3b** in Gunn and normal rats: (a) HPLC of bile collected just before ($t = 0$) and 12 and 30 min after intravenous injection of **3b** (~ 0.25 mg) in a Gunn rat; (b) chromatograms of bile collected before and 12 min after similar injection in a Sprague-Dawley rat; (c) concentration/time excretion curves for the mono- (■) and diglucuronide (●) of **3b** in normal rats (the monoglucuronide plot is the mean of three experiments; because of overlap of the diglucuronide HPLC peak with those of endogenous bilirubin monoglucuronides, the excretion curve for the diglucuronide is only approximate and data from a single rat are plotted). Each set of biliary excretion curves was normalized ($\times 10$) to the peak area of the largest HPLC peak.

hydrogen-bonded.²⁰ However, to accommodate the hydrogen bonding, the dipyrinones are twisted out of planarity and the two triads of hydrogen bonds are severely distorted (weakened). Examination of Dreiding models of **5a** suggests that the dipyrinone chromophores can return to planarity with loss of distortion if just one of the carboxyl groups is tightly hydrogen-bonded and the other is free, analogous to the preferred conformation calculated for acetylenic bilirubin **3a** (Figure 4).

On silica thin-layer chromatography, **5a** was found to be much more polar than mesobilirubin XIII α , as expected for a bilirubin with weaker internal hydrogen bonding or with only one carboxyl hydrogen-bonded. However, unexpectedly, on reversed-phase HPLC it had a very much longer retention time than mesobilirubin XIII α . The reason for this anomalous behavior, which complicated the analysis of bile samples, is unclear. It may be caused by di-*n*-octylamine in the HPLC eluent forming a hydrophobic complex with **5a** by intercalating into and strengthening the network of intramolecular hydrogen bonds. Bilirubin has been shown to form such a complex with diisopropylamine.⁹ Consistent with this interpretation, the dianion of **5a** showed an unusually high affinity for monovalent cations, which made isolation of the free acid difficult.

When **5a** was injected into Gunn rats, it was excreted rapidly in bile unchanged (Figure 9a). In normal rats it was excreted partly unchanged and partly as two very much more polar metabolites, of which the most polar overlapped the endogenous bilirubin diglucuronide peak (Figure 9b). Hydrolyses of bile samples with NaOH and β -glucuronidase were consistent with the assumption that the metabolites are the mono- and diglucuronide of **5a**. HPLC of bile samples subjected to alkaline methanolysis revealed the presence of two main peaks not present in similarly treated control bile (Figure 9c). These were

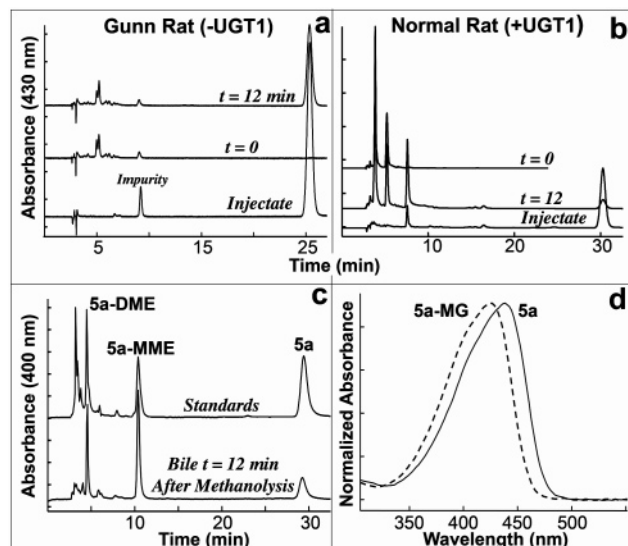


Figure 9. Hepatic metabolism and biliary excretion of **5a** in Gunn and normal rats: (a) HPLC of bile collected just before ($t = 0$) and 12 min after intravenous injection of **5a** (~ 0.25 mg) in a Gunn rat; (b) chromatograms of bile collected before ($t = 0$) and 12 min after similar injection in a Sprague-Dawley rat. The two peaks in the $t = 0$ chromatogram are the endogenous diglucuronide and unresolved monoglucuronides of bilirubin. Chromatograms shown in panels a and b were run on different instruments with different columns, which accounts for the somewhat different retention times for **5a** in the two panels. Panel c shows chromatograms of **5a**-dimethyl ester after partial hydrolysis (standards) and of a sample of bile collected 12 min after injection of **5a** in a Sprague-Dawley rat and treated by alkaline methanolysis. Panel d shows the normalized absorption spectra of **5a** (solid line) and its monoglucuronide (dashed line) captured during HPLC of bile.

identified as the mono and dimethyl ester of **5a** by HPLC/UV–vis comparison with authentic samples, supporting the identification of the two metabolites as mono- and diacylglyceronides. Thus, the metabolism of **5a** in the rat is similar to that of exploded bilirubin **3a** and different from that of its homologue mesobilirubin XIII α in that it is a substrate for a UGT1 enzyme, presumably UGT1A1, but glucuronidation is not essential for its biliary excretion. In contrast to our observations on exploded bilirubins **3a** and **3b**, glucuronidation of **5a** caused only a hypsochromic shift of ~ 13 nm without a major change in the shape of the absorption band (Figure 9d).

Molecular dynamics calculations have shown that as the propanoic acid side chains of mesobilirubin are progressively lengthened, the most stable conformation becomes a folded structure in which intramolecular hydrogen bonding of the carboxyl groups is maintained.²⁰ However, in going from propanoic to hexanoic, gauche butane and other intramolecular nonbonded steric interactions in the alkanic acid chains increase. These destabilize and weaken the hydrogen bonding so that the triad of hydrogen bonds in which each carboxyl group is involved becomes more distorted, less planar, and less compact than the similar triads in bilirubin and mesobilirubin XIII α . This is exemplified in Figure 10, which shows the global energy minimum conformation for **5e**, in which the acid side chains of mesobilirubin XIII α have been lengthened by three carbon units from propanoic to hexanoic.

The hepatobiliary excretion of **5c**, with butanoic acid side chains, was similar to that of mesobilirubin XIII α (data not shown). It was not excreted significantly in bile when injected into Gunn rats but appeared promptly in bile in normal rats as two acylglucuronide metabolites. However, **5d** and **5e**, with even longer side chains, were excreted unchanged into bile in Gunn

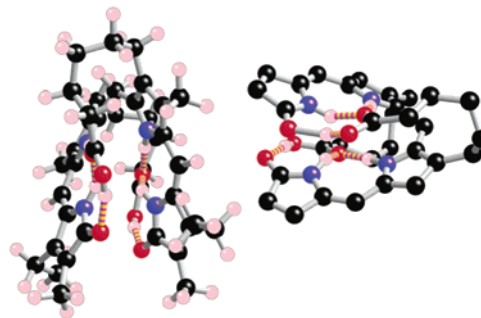


Figure 10. Ball-and-stick representations of the minimum energy conformation of **5e**: (left) ridge-tile orientation; (right) partial structure, with some hydrogens and β -substituents removed, showing hydrogen bonding of the carboxyl groups. Striped bonds represent hydrogen bonds.

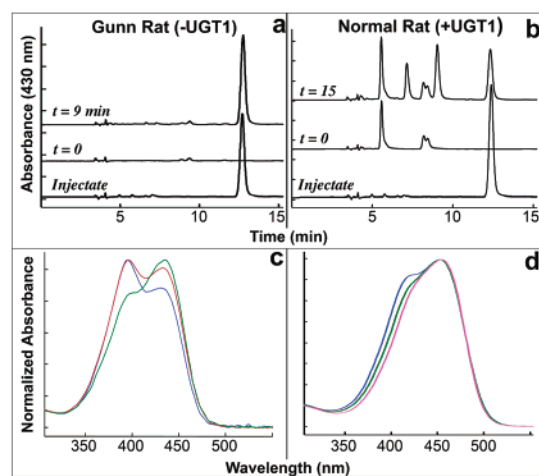


Figure 11. Hepatic metabolism and biliary excretion of **5e** in Gunn and normal rats: (a) HPLC of bile collected just before ($t = 0$) and 9 min after intravenous injection of **5e** (~ 0.25 mg) in a Gunn rat; (b) chromatograms of bile collected before ($t = 0$) and 15 min after similar injection in a Sprague-Dawley rat. The prominent peaks in the $t = 0$ chromatogram are the endogenous diglucuronide and overlapping monoglucuronides of bilirubin. Panel c shows the normalized absorption spectra of **5e** (green), **5e**-monoglucuronide (red), and **5e**-diglucuronide (blue). Panel d shows, for comparison, normalized absorption spectra of bilirubin (purple), bilirubin monoglucuronides (green), and bilirubin diglucuronide (blue) under the same conditions.

rats and yet as a mixture of intact pigment and acylglucuronides in normal rats, just like the bis-acetic homologue **5a** and the acetylenic bilirubin **3a**. This is shown in Figure 11 for **5e** with a hexanoic acid side chain. Figure 11a shows HPLC chromatograms of Gunn rat bile before and 9 min after injecting the pigment intravenously; Figure 11b shows similar chromatograms of bile from a normal rat before and 15 min after administration of **5e**. The two metabolite peaks near 7 and 9 min appearing along with unchanged pigment in bile from Sprague-Dawley rats were identified as glucuronides by NaOH and β -glucuronidase hydrolysis. Glucuronidation of **5e** led to pronounced changes in the absorption spectrum (Figure 11c) that were much greater than those seen on glucuronidation of **5a** (Figure 9b) or bilirubin (Figure 11d). Presumably nonbonded interactions within the hexanoic side chains of **5e** coupled with the loosening of hydrogen bonding on glucuronidation of the carboxyl groups allow a greater contribution of chromophore conformations other than the folded conformation shown in Figure 10.

Diacetylenic Bilirubins 4a and 4b. The exploded bilirubin **4a** has dipyrrinone chromophores identical to those of the monoacetylenic bilirubin **3a** and of mesobilirubin XIII α , but they are forced further apart by the dual linear dialkyne linkage.

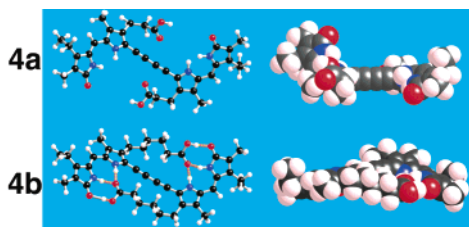


Figure 12. Ball-and-stick (left) and space-filling (right) models of global minimum energy conformations of **4a** and **4b**. Striped bonds are hydrogen bonds.

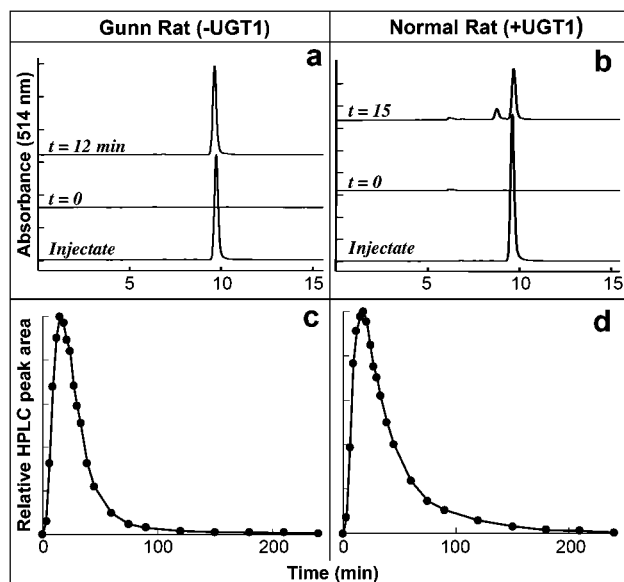


Figure 13. Hepatobiliary excretion of **4a** in Gunn and Sprague-Dawley rats: (a) HPLC of bile before ($t = 0$) and 12 min after intravenous injection of **4a** (~ 0.25 mg) in a Gunn rat; (b) HPLC of bile before ($t = 0$) and 15 min after similar injection in a Sprague-Dawley rat. Panels c and d show biliary excretion curves for unchanged **4a** in Gunn (mean of two experiments) and Sprague-Dawley (mean of three experiments) rats, respectively.

Rotation of the dipyrinone “blades” about the dialkyne axis is possible, but intramolecular hydrogen bonding between the carboxyl groups and lactam and pyrrole NH/CO functions is sterically impossible. Intramolecular hydrogen bonding between the two COOH groups is possible in conformations in which the two dipyrinone chromophores have a syn disposition. However, the global energy minimum conformation for **4a** predicted by molecular dynamics force field calculations shows two well-separated dipyrinone chromophores with an anti disposition (Figure 12).¹⁸ When injected into Gunn rats (Figure 13a,c) and normal rats (Figure 13b,d), **4a** was excreted rapidly in bile in intact form. The fraction of unchanged **4a** excreted in bile in 240 min was 0.54 ± 0.059 (mean of five experiments: two Gunn and three Sprague-Dawley rats). Thus, **4a**, in which neither of the propanoic acid side chains is hydrogen-bonded, is cholephilic and does not require conjugation for excretion. However, in normal rats a relatively small proportion of a single metabolite, more polar than the parent compound, was detected (Figure 13b). This metabolite has an absorbance spectrum identical to that of the parent compound. Treatment of bile samples with NaOH and β -glucuronidase (not shown) led to its disappearance and enhancement of the parent **4a** peak. Thus, the metabolite appears to be a glucuronide, presumably the monoglucuronide, of **4a**.

Diacetylenic bilirubin **4b** has geometry similar to that of **4a**, but the greater length of the carboxylic side chains permits re-

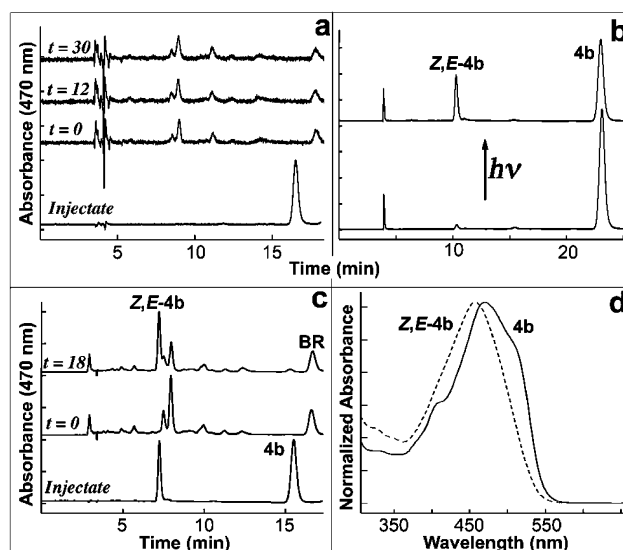
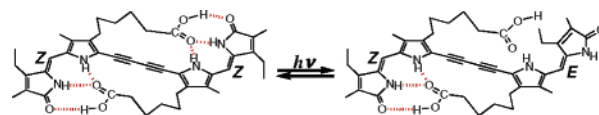


Figure 14. Hepatobiliary excretion of **4b** and its *Z,E* isomer in the Gunn rat: (a) HPLC of bile before ($t = 0$) and 12 and 30 min after injection of **4b** (~ 0.25 mg) in a Gunn rat, where the scale for the bile chromatograms is expanded compared to that of the injectate; (b) HPLC of **4b** in DMSO before and after exposure to blue light; (c) HPLC of bile before ($t = 0$) and 18 min after injection of a mixture (injectate) of **4b** and *Z,E*-**4b** in a Gunn rat (BR indicates endogenous bilirubin); (d) normalized absorbance spectra of **4b** and *Z,E*-**4b**.

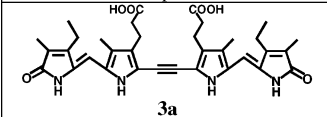
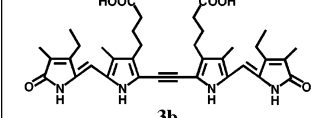
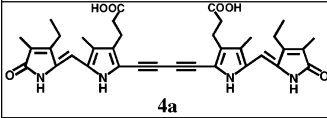
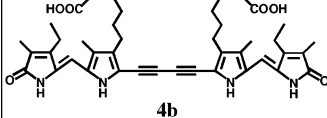
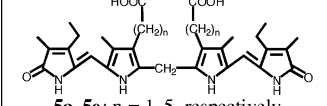
Scheme 2. Photoisomerization of **4b**



establishment of intramolecular hydrogen bonding. The computed global minimum-energy conformation for this compound is an almost planar structure, with snug hydrogen bonding of its carboxyl groups (Figure 12). No significant biliary excretion of **4b**, either as metabolites or as intact pigment, was detected in Gunn rats within the 4 h experimental time period after its intravenous injection (Figure 14a). Yet, analyses of serum indicated that the substance was rapidly cleared from the circulation by the liver. The same lack of excretion of intact pigment or glucuronides was also observed in normal rats. This suggests that **4b** is not a substrate for UGT1A1 or other phase 2 enzymes in rat liver. Like bilirubin, **4b** is too lipophilic to be eliminated efficiently in bile but, unlike bilirubin or mesobilirubin XIII α , is not metabolized rapidly to glucuronide or other metabolites with intact dipyrinone chromophores.

Since hydrogen bonding prevents the elimination of **4b**, disruption of hydrogen bonding might be expected to facilitate its excretion. One way to achieve this would be by *Z* \rightarrow *E* isomerization of one of the exocyclic double bonds of its dipyrinone chromophores (Scheme 2).²⁶ Similar isomerization of bilirubin is known to facilitate its biliary excretion as unchanged *4Z,15E*- and *4E,15Z*-bilirubin in the rat.²⁷ Exposure of **4b** in DMSO under argon to blue light led to rapid appearance of a new more polar peak on HPLC (Figure 14b) with maximum absorbance (Figure 14d) shifted to wavelengths shorter than that of **4b**. This peak reverted to the parent isomer on standing in solution in the dark at room temperature. Although this photoproduct was not characterized further, there can be little doubt that it is the *Z,E* isomer of **4b**. Dilution of a DMSO solution of **4b** that had been irradiated close to the *Z,Z/Z,E* photostationary state in rat serum followed by centrifugation to remove a small quantity of precipitated material yielded a

Table 1. Summary of the Hepatobiliary Metabolism of Mono- and Diacetylenic Bilirubins and Mesobilirubin XIII α Homologues in Normal and Gunn Rats

Compound	Gunn rat (- UGT1)	Wild-type rat (+ UGT1)
 3a	Excreted unchanged	Excreted partly unchanged; partly as acyl glucuronides
 3b	Not excreted	Excreted as acyl glucuronides
 4a	Excreted unchanged	Excreted unchanged
 4b	Not excreted	Not excreted
 5a–5e; n = 1–5, respectively	n = 1 Excreted unchanged n = 2,3 Not excreted n = 4,5 Excreted unchanged	n = 1 Excreted partly unchanged; partly as acyl glucuronides n = 2,3 Excreted as acyl glucuronide n = 4,5 Excreted partly unchanged; partly as acyl glucuronides

solution containing 38% *Z,E*-**4b** and 62% *Z,Z*-**4b** based on relative HPLC peak areas of the two isomers measured at 470 nm. When this solution was injected intravenously into a Gunn rat, prominent peaks corresponding to unchanged *Z,E* isomer were detectable in HPLC chromatograms of bile (Figure 14c), whereas only trace peaks of the parent *Z,Z* isomer were present. When bile samples containing the putative *Z,E* isomer were exposed very briefly to blue light or were allowed to stand at room temperature, the *Z,E* peak disappeared with growth of the *Z,Z* peak. Thus, the *Z,E* isomer of **4b** is taken up by the liver and, in contrast to the *Z,Z* isomer, is excreted into bile, albeit rather inefficiently. This is consistent with the hypothesis that it is the potential for compact, tight internal hydrogen bonding in **4b** that prevents its hepatobiliary excretion in intact form, as it does in **3b** and in bilirubin. Space-filling models of **4a** and **4b** (Figure 12) reveal the lipophilic surface of **4b** and the poor solvent exposure of the polar carboxyl groups in **4b** compared to **4a**.

Discussion

The observations of this study are summarized in Table 1. They show that the hepatic metabolism of the exploded bilirubins **3** and **4** and of the mesobilirubin XIII α homologues **5a–e** is remarkably sensitive to small changes in the lengths of the carboxyl side chains within each series. The experimental observations would be difficult to rationalize solely on the basis of the usual two-dimensional linear structural representations depicted in Table 1. For example, compounds **3a** and **3b**, which differ by only one methylene unit in the lengths of their acid side chains, might be expected to undergo rather similar metabolism and transport in the Gunn rat, and little difference would be expected between **5c** and **5d**, which differ in a similar way. Furthermore, from a comparison of the linear structures in Table 1 with those of bilirubin (**1**) and biliverdin (**2**) it would be difficult to predict which would be excretable intact in the Gunn rat or which would require glucuronidation for biliary excretion in wild-type animals. However, the experimental observations become more explicable and comprehensible when the preferred conformations and potential intramolecular hydrogen-bonding interactions of the compounds are considered.

Taken together, the observations are consistent with the premise that particular conformations of tetrapyrrolic dipyrinone pigments are favored in vivo and that the ability of the COOH groups to form intramolecular hydrogen bonds inhibits excretion into bile and favors glucuronidation by UGT1A1. Overall, the observed metabolic behavior correlates well with predictions based on preferred conformations derived from molecular dynamics calculations. This is not to say that the most stable conformer derived from calculations and shown to be present in organic solvents by heteronuclear NOE NMR experiments also prevails in vivo where carboxyl groups may be ionized and hydrogen bonding to water may be important. But the observations clearly indicate that the potential for intramolecular hydrogen bonding of the carboxyl/carboxylate groups in these compounds has a major influence on their hepatobiliary disposition and propensity for glucuronidation. What might appear to be small inconsequential structural changes can have a significant effect on metabolism if they stress, disrupt, or hinder intramolecular hydrogen bonding. For example, in **3a** simultaneous tight hydrogen bonding of each carboxyl group to a contralateral dipyrinone is frustrated by the linear separation imposed by the acetylenic spacer. This suffices to make **3a** polar enough to be excreted in bile without the need for conjugation. In contrast, extending the length of each carboxyl side chain by just one carbon to give **3b** facilitates tight and simultaneous intramolecular hydrogen bonding of both carboxyl groups. Consequently, this compound, like bilirubin and mesobilirubin XIII α , requires conjugation (glucuronidation) for excretion in bile.

Possible partial exceptions are the diacetylenic compounds **4a** and **4b**. The COOH groups in **4a** are sterically unable to form the usual bilirubin-type hydrogen bonds. As expected, this compound was excreted promptly in unchanged form in Gunn and wild-type rats. However, in the latter a relatively small proportion of a glucuronide, presumably the monoglucuronide, was formed. This suggests that intramolecular hydrogen bonding of the COOH groups in bilirubins to contralateral NH and lactam groups is not an absolute requirement for glucuronidation but heavily favors it. It is also possible that intramolecular hydrogen

bonding of the two COOH groups in **4a** to each other, rather than to NH and lactam groups, favors acyl glucuronidation. This would be consistent with our detection of only a single glucuronide of **4a** rather than a mixture of two (mono- and diglucuronide) because the intramolecular hydrogen bonding would be disrupted once one COOH had been glucuronidated. Intramolecular hydrogen bonding between the two COOH groups in bilirubin is sterically unfavorable but possible for the two COOH groups in **4a**, as shown by molecular models.

In its fully hydrogen-bonded preferred conformation, **4b** has a compact planar shape in which the polar functions are well-shielded on one side by the central core of contiguous carbon atoms and on the other by hydrophobic substituents (Figure 12). Not surprisingly, **4b** was not excreted in bile when administered to Gunn rats but neither was it metabolized to glucuronides and excreted in bile as such in normal rats. The reason for this is unclear. It could reflect a low affinity of UGT1A1 for **4b** or the inability of the enzyme cofactor, uridine diphosphoglucuronic acid, to access the carboxyl groups. Notably, however, when hydrogen bonding of one of the carboxyl groups was prevented by photochemical *Z* → *E* isomerization of a dipyrinone double bond (Scheme 2), the compound became excretable in bile without the need for hepatic conjugation (Figure 14).

Numerous studies have stressed the importance of the “ridge–tile” conformation in the metabolism and glucuronidation of bilirubin. Our observations show that the ridge–tile shape of bilirubin per se is not important. For example, **3b**, which has an almost planar preferred conformation and quite different dimensions from bilirubin, was metabolized and glucuronidated in an identical manner to the natural pigment. What seems to be important is the presence of a planar potentially hydrogen-bonded motif that can slot into the catalytic site of a UGT1 enzyme located near the exterior surface of the protein rather than deep within.

For bilirubin and the dicarboxylic acids we studied, as well as their respective monoglucuronides and probably many other carboxylic acids too, there appears to be competition or interplay within the liver between direct excretion into bile (phase 0 metabolism) and glucuronidation (phase 2 metabolism). The balance between glucuronidation and direct efflux may be one of competing rate processes. Exposed carboxyl groups seem to favor the direct route of elimination, whereas the potential for carboxyl infolding by hydrogen bonding seems to favor glucuronidation. Irrespective of whether or not a compound is a UGT substrate, if direct elimination is fast enough, there may not be enough time and would be no need for significant glucuronidation to occur, especially if the affinity of the compound for UGT is low. Therefore, failure to observe glucuronidation of a particular acid *in vivo* does not necessarily mean that it is not a UGT substrate or would not undergo glucuronidation if incubated long enough under static conditions *in vitro* with liver microsomes or recombinant enzymes and appropriate cofactors. Conversely, the demonstration that a compound undergoes glucuronidation in an *in vitro* system does not necessarily imply that that pathway will predominate *in vivo*. A major weakness of *in vitro* systems for predicting *in vivo* metabolism is that they do not reveal what fraction of a test compound would be eliminated unchanged in bile or the relative importance of phase 0 and phase 2 elimination pathways. Although our studies were done in the rat, the same general principals are likely to hold in humans and other mammals because the metabolism of bilirubin is very similar in most mammals.

Experimental Section

Synthesis, characterization, and analytical data (including ^{13}C and ^1H NMR, IR, and UV–vis spectra, combustion analyses, and/or high-resolution MS) for all tetrapyrrole pigments used in this study have been reported previously.^{17,18,20} Animal procedures, HPLC methods, and the provenance of the animals used also have been described in detail previously.²⁸ All animal studies were in compliance with institutional guidelines and approval requirements. For metabolism studies, each pigment (~0.25 mg, accurately weighed on a microbalance) was dissolved in 0.1 mL of dimethyl sulfoxide (DMSO) or argon-degassed 0.1 M NaOH and the optically clear solution was slowly and quantitatively diluted into 1 mL of rat serum using a finely drawn out Pasteur pipet. The final solution was microfuged briefly, two 20- μL aliquots were taken from the supernate for HPLC analysis, and the remainder was injected intravenously over ~60 s into the femoral vein of a male rat (>250 g) fitted with a short (7.5 cm) in-dwelling PE-50 biliary cannula for rapid collection of bile. Hydration and bile flow were maintained by infusion of a bile salt/lipid solution.²⁸ Bile was collected in 20- μL aliquots into glass tubes and flash-frozen immediately with dry ice, and bile flow rates were estimated gravimetrically. Frozen samples were stored at $-70\text{ }^\circ\text{C}$ pending HPLC analysis, when they were mixed with 80 μL of eluent and microfuged. A 50- μL aliquot of the supernate was injected without delay via a 20- μL sample loop onto a C18 reversed-phase column, and eluting peaks were detected with a diode array detector at their absorption maxima and at 450 nm, the absorption maximum for bilirubin. Blood samples were collected from a nick in the tail vein and allowed to clot, and 20- μL samples were taken for HPLC analysis as above. All procedures involving pigment solutions, collection of blood and bile samples, and HPLC analyses were done under red or orange safelights in a darkroom. Metabolites were identified as acylglucuronides if they met all three of the following criteria: formed in wild type rats but not in UGT1A-deficient Gunn rats; hydrolyzed to parent aglycone by β -glucuronidase; hydrolyzed to parent aglycone by NaOH. Further evidence for the identification of metabolites of **5a** as acylglucuronides was their conversion to known methyl esters of **5a** by alkaline methanolysis. β -Glucuronidase hydrolysis of glucuronides in bile was done by adding 40 μL of glucuronidase solution (prepared by adding 1 mL of water to 1000 units of Sigma bacterial *E. coli* type II or VIIa glucuronidase) to 20 μL of bile, incubating at $37\text{ }^\circ\text{C}$ in the dark for 60 min, mixing with 140 μL of HPLC eluent, and microfuging to remove protein. The supernate (20 μL) was chromatographed at once. For NaOH hydrolysis, 20- μL samples of bile were mixed with 10 μL of 1.0 M NaOH, followed after 3 min by 10 μL of 1.0 M HCl and 80 μL of HPLC eluent. The final mixture was microfuged and the supernate analyzed by HPLC without delay. In some experiments neutralization with HCl was omitted. Alkaline methanolysis of bile containing glucuronides of **5a** was done by mixing bile (20 μL) with 0.5 mL of MeOH and 0.5 mL of KOH/MeOH (2 g w/v %) followed after 1 min by addition of CHCl_3 (0.5 mL) and 0.4 M glycine–HCl buffer (pH 2.4, 0.5 mL). The mixture was shaken and microfuged, and the residue remaining after evaporation of the CHCl_3 phase under argon was dissolved in HPLC eluent for HPLC. Reference **5a** monomethyl ester was obtained by heating **5a**-dimethyl ester in KOH/MeOH (1 g w/v %) for 60 min at $60\text{ }^\circ\text{C}$. For preparation of *Z,E*-**4b**, 0.5 mg *Z,Z*-**4b** was dissolved in 0.1 mL of argon-degassed DMSO and exposed in a small glass Pasteur tube for 15 min to light from a 20-W Westinghouse Special Blue F20T12/BB fluorescent tube with maximum output at ~430–460 nm. The solution was immediately diluted into 1 mL of ice-cold rat serum and centrifuged for 10 min at $4\text{ }^\circ\text{C}$, and the red supernate was used for intravenous injection of a Gunn rat. The isocratic HPLC eluent used throughout was 0.1 M di-*n*-octylamine acetate (prepared from Aldrich di-*n*-octylamine and glacial acetic acid) in MeOH containing from 2–8% water. The column was a Beckman-Altex Ultrapshere-IP 5 μm C-18 ODS column (25 cm \times 0.46 cm) fitted with a similarly packed precolumn (4.5 cm \times 0.46 cm), and eluted peaks were detected with a Hewlett-

Packard multiwavelength diode array detector. Parent and metabolite peaks were monitored at the absorption maximum of the parent compound in the HPLC eluent, and HPLC peak areas were measured using HP ChemStation software. For quantitation, the approximation was made that the absorbances of parent and metabolites were identical at that wavelength. Biliary excretion curves were derived by plotting integrated HPLC peak areas normalized to the maximum peak area. The fraction of the injected dose excreted was estimated by comparing the area under the biliary excretion curve (HPLC peak area versus time), adjusted for total bile volume excreted, with the HPLC peak area of the pigment in a 20- μ L sample of the original serum solution injected into the rat. Areas under biliary excretion curves were determined using Un-Scan-It software (Silk Scientific, Inc., Orem, UT). Except where noted otherwise, ball-and-stick models are based on coordinates generated by Sybyl molecular dynamics calculations and were drawn using CrystalMaker (version 6.3.10 for Mac OS-X, CrystalMaker Software Ltd., Yarnton, U.K.).

Acknowledgment. We thank Drs. Bin Tu and David. P. Shrout for syntheses of the compounds used in this study, Drs. Brahmananda Ghosh and Richard Person for Sybyl molecular dynamics calculations, Professor P. Manitto (University of Milan) for providing the crystal structure coordinates of bilirubin diisopropylammonium salt,⁹ and Wilma Norona for technical assistance. The work was supported by Grants HD-17779 and DK-26307 from the National Institutes of Health.

References

- el Tayar, N.; Mark, A. E.; Vallat, P.; Brunne, R. M.; Testa, B.; van Gunsteren, W. F. Solvent-dependent conformation and hydrogen-bonding capacity of cyclosporin A: evidence from partition coefficients and molecular dynamics simulations. *J. Med. Chem.* **1993**, *36*, 3757–3764.
- Gourley, G. R. Bilirubin metabolism and kernicterus. *Adv. Pediatr.* **1997**, *44*, 173–229.
- Owens, I. S.; Basu, N. K.; Banerjee, R. UDP-glucuronosyltransferases: gene structures of UGT1 and UGT2 families. *Methods Enzymol.* **2005**, *400*, 1–22.
- ABC transporters are both enzymes and membrane transporters. In the nomenclature introduced by Holland and Blight the term “allocrite” refers to compounds whose passage across membranes is facilitated by an ABC transporter: Holland, I. B.; Blight, M. A. ABC-ATPases, adaptable energy generators fuelling transmembrane movement of a variety of molecules in organisms from bacteria to humans. *J. Mol. Biol.* **1999**, *293*, 381–399.
- Dietrich, C. G.; Geier, A.; Oude, Elferink, R. J. P. ABC of oral bioavailability: transporters as gatekeepers in the gut. *Gut* **2003**, *52*, 1788–1795.
- Nies, A. T.; Keppler, D. The apical conjugate efflux pump ABCC2 (MRP2). *Pfluegers Arch.*, in press.
- Chandra, P.; Brouwer, K. L. The complexities of hepatic drug transport: current knowledge and emerging concepts. *Pharm. Res.* **2004**, *21*, 719–35.
- Bonnett, R.; Davies, J. E.; Hursthouse, M. B.; Sheldrick, G. M. The structure of bilirubin. *Proc. R. Soc. London, Ser. B.* **1978**, *202*, 249–268.
- Mugnoli, A.; Manitto, P.; Monti, D. Structure of di-isopropylammonium bilirubinate. *Nature* **1978**, *273*, 568–569.
- Hagiwara, Y.; Sugishima, M.; Takahashi, Y.; Fukuyama, K. Crystal structure of phycocyanobilin:ferredoxin oxidoreductase in complex with biliverdin IX α , a key enzyme in the biosynthesis of phycocyanobilin. *Proc. Natl. Acad. Sci. U.S.A.* **2006**, *103*, 27–32.
- Wagner, U. G.; Müller, N.; Schmitzberger, W.; Falk, H.; Kratky, C. Structure determination of the biliverdin apomyoglobin complex: Crystal structure analysis of two crystal forms at 1.4 and 1.5 Å resolution. *J. Mol. Biol.* **1995**, *247*, 326–337.
- Lightner, D. A.; Holmes, D. L.; McDonagh, A. F. On the acid dissociation constants of bilirubin and biliverdin. pK_as from ¹³C-NMR spectroscopy. *J. Biol. Chem.* **1996**, *271*, 2397–2405.
- McDonagh, A. F.; Lightner, D. A.; Kar, A. K.; Norona, W. S. Hepatobiliary excretion of biliverdin isomers and C10-substituted biliverdins in Mrp2-deficient (TR⁻) rats. *Biochem. Biophys. Res. Commun.* **2002**, *293*, 1077–1083.
- Kogan, M. J.; Mora, M. E.; Awruch, J.; Delfino, J. M. Probing the conformation of bilirubins with monopropionic analogs: a biological, spectroscopic, and molecular modeling study. *Bioorg. Med. Chem.* **1998**, *6*, 151–161.
- McDonagh, A. F.; Lightner, D. A.; Nogales, D. F.; Norona, W. S. Biliary excretion of a stretched bilirubin in UGT1A1-deficient (Gunn) and Mrp2-deficient (TR⁻) rats. *FEBS Lett.* **2001**, *506*, 211–215.
- (a) By analogy with earlier usage,^{16b,c} we use the term “exploded” bilirubins to distinguish expanded bilirubins in which the separation of the two dipyrinone chromophores has been increased by insertion of a rigid spacer group, in this case alkyne groups, in place of the normal C10–CH₂ linkage. (b) Miljanic, O. S.; Han, S.; Holmes, D.; Schaller, G. R.; Vollhardt, K. P. C. Hindered rotation in an “exploded” biphenyl. *Chem. Commun.* **2005**, 2606–2608. (c) Houk, K. N.; Scott, L. T.; Rondan, N. G.; Spellmeyer, D. C.; Reinhardt, G.; Hyun, J. L.; Decicco, G. J.; Weiss, R.; Chen, M. H. M.; Bass, L. S.; Clardy, J.; Jørgensen, F. S.; Eaton, T. A.; Sarkozi, V.; Petit, C. M.; Ng, L.; Jordan, K. D. Pericyclics: exploded cycloalkanes with unusual orbital interactions and conformational properties. Mm2 and Sto-3G calculations, X-ray crystal-structures, photoelectron-spectra, and electron transmission spectra. *J. Am. Chem. Soc.* **1985**, *107*, 6556–6562.
- Tu, B.; Ghosh, B.; Lightner, D. A. A new class of linear tetrapyrroles: acetylenic 10,10a-didehydro-10a-homobilirubins. *J. Org. Chem.* **2003**, *68*, 8950–8963.
- Tu, B.; Ghosh, B.; Lightner, D. A. Novel linear tetrapyrroles: hydrogen bonding in diacetylenic bilirubins. *Monatsh. Chem.* **2004**, *135*, 519–541.
- Chen, Q.; Huggins, M. T.; Lightner, D. L.; Norona, W.; McDonagh, A. F. Synthesis of a 10-oxo-bilirubin. Effects of the oxo group on conformation, transhepatic transport and glucuronidation. *J. Am. Chem. Soc.* **1999**, *121*, 9253–9264.
- Trull, F. R.; Person, R. V.; Lightner, D. A. Conformational analysis of symmetric bilirubin analogues with varying length alkanolic acids. Enantioselectivity by human serum albumin. *J. Chem. Soc., Perkin Trans. 2* **1997**, 1241–1250.
- Clarke, D. J.; Keen, J. N.; Burchell, B. Isolation and characterisation of a new hepatic bilirubin UDP-glucuronosyltransferase: Absence from Gunn rat liver. *FEBS Lett.* **1992**, *299*, 183–186.
- Sato, H.; Aono, S.; Kashiwamata, S.; Koiwai, O. Genetic defect of bilirubin UDP-glucuronosyltransferase in the hyperbilirubinemic Gunn rat. *Biochem. Biophys. Res. Commun.* **1991**, *177*, 1161–1164.
- Jansen, P. L.; Peters, W. H.; Lamers, W. H. Hereditary chronic conjugated hyperbilirubinemia in mutant rats caused by defective hepatic anion transport. *Hepatology* **1985**, *5*, 573–579.
- Paulusma, C. C.; Oude Elferink, R. P. J. The canalicular multispecific organic anion transporter and conjugated hyperbilirubinemia in rat and man. *J. Mol. Med.* **1997**, *75*, 420–428.
- Person, R. V.; Peterson, B. R.; Lightner, D. A. Bilirubin conformational analysis and circular dichroism. *J. Am. Chem. Soc.* **1994**, *116*, 42–59.
- McDonagh, A. F.; Palma, L. A.; Trull, F. R.; Lightner, D. A. Phototherapy for neonatal jaundice. Configurational isomers of bilirubin. *J. Am. Chem. Soc.* **1982**, *104*, 6865–6867.
- Lightner, D. A.; McDonagh, A. F. Molecular mechanisms of phototherapy for neonatal jaundice. *Acc. Chem. Res.* **1984**, *17*, 417–424.
- Woydziak, Z. R.; Boiadjev, S. E.; Norona, W. S.; McDonagh, A. F.; Lightner, D. A. Synthesis and hepatic transport of strongly fluorescent cholephilic dipyrinones. *J. Org. Chem.* **2005**, *70*, 8417–8423.

JM0609521